doi: 10.32023/0001-5237/71.3.1

ACTA ASTRONOMICA
Vol. **71** (2021) pp. 189–204

Over 24 000 δ Scuti Stars in the Galactic Bulge and Disk from the OGLE Survey*

I. Soszyński[1], P. Pietrukowicz[1], J. Skowron[1], A. Udalski[1], M. K. Szymański[1], D. M. Skowron[1], R. Poleski[1], S. Kozłowski[1], P. Mróz[1], K. Ulaczyk[2,1], K. Rybicki[1], P. Iwanek[1], M. Wrona[1] and M. Gromadzki[1]

[1] Astronomical Observatory, University of Warsaw, Al. Ujazdowskie 4, 00-478 Warszawa, Poland
[2] Department of Physics, University of Warwick, Gibbet Hill Road, Coventry, CV4 7AL, UK

Received November 3, 2021

ABSTRACT

We present the largest collection of δ Scuti-type stars in the Milky Way. Together with the recently published OGLE collection of δ Sct variables in the inner Galactic bulge, our sample consists of 24 488 objects distributed along the Milky Way plane, over Galactic longitudes ranging from about -170° to $+60^\circ$. The collection data include the *I*- and *V*-band time-series photometry collected since 1997 during the OGLE-II, OGLE-III, and OGLE-IV surveys. We show the on-sky distribution of δ Sct stars in the Galactic bulge and disk, discuss their period, luminosity and amplitude distributions, present Petersen diagram for multimode pulsators, distinguish 34 δ Sct stars in eclipsing and ellipsoidal binary systems, and list probable members of globular clusters.

Key words: *Stars: variables: delta Scuti – Stars: oscillations – Galaxy: bulge – Galaxy: disk – Catalogs*

1. Introduction

δ Sct variables constitute a diverse class of short-period pulsating stars located in the lower part of the classical instability strip in the Hertzsprung-Russell diagram. These objects cover a wide range of stellar evolutionary stages: young stellar objects during their contraction toward the main sequence, stars with core hydrogen burning on the main sequence, subgiants evolving off the main sequence, and blue stragglers known as SX Phoenicis variables†. δ Sct pulsators can be monoperiodic

*Based on observations obtained with the 1.3-m Warsaw telescope at the Las Campanas Observatory of the Carnegie Institution for Science.

†In this paper, we refer to SX Phe stars as one of the subgroups of δ Sct stars.

or multiperiodic, with radial or nonradial modes excited, and the pulsation periods ranging from approximately 0.03 d to 0.3 d. Like other types of classical pulsators (Cepheids and RR Lyrae stars), δ Sct variables follow period–luminosity relations, which makes them potentially useful as distance indicators.

The number of known δ Sct stars in the Milky Way has grown rapidly in recent years, mostly thanks to the large-scale photometric sky surveys. The catalog of all δ Sct variables known in January 2000 compiled by Rodríguez *et al.* (2000) consisted of 636 objects. This number has increased by a factor of ≈ 50 since then. So far, the largest samples of the Galactic δ Sct stars have been included in the ASAS-SN catalogue of variable stars (≈ 8400 objects, Jayasinghe *et al.* 2020) and in the Zwicky Transient Facility Catalog of Periodic Variable Stars ($\approx 15\,000$ objects, Chen *et al.* 2020).

Recently, Pietrukowicz *et al.* (2020) published a collection of 10 092 δ Sct stars toward the Galactic bulge detected in the Optical Gravitational Lensing Experiment (OGLE) photometric database. About 97% of this sample were new discoveries. In this paper, we present an extension of the Pietrukowicz *et al.* (2020) catalog to include newly detected δ Sct stars in the Galactic disk and outer bulge – regions of the sky photometrically monitored by the OGLE Galaxy Variability Survey (GVS). Our extended collection contains over 24 000 δ Sct variables and is currently the largest sample of such objects in the Milky Way. This is also a part of the OGLE Collection of Variable Stars (OCVS) consisting of over a million carefully selected and classified variable stars of various types. Among others, we recently published extensive catalogs of Cepheids (Udalski *et al.* 2018, Soszyński *et al.* 2020) and RR Lyr stars (Soszyński *et al.* 2019) in the Milky Way.

The outline of the paper is as follows. In the next section, we present the OGLE observations and data reduction pipeline. Section 3 provides a description of the procedures used for the identification and classification of variable stars in the OGLE photometric database. In Section 4, we summarize the OGLE collection of δ Sct stars in the Galactic bulge and disk and present their on-sky distribution. In Section 5, we cross-match our sample to external catalogs and estimate its completeness. Particularly interesting cases of δ Sct variables: multimode pulsators, binary systems containing pulsating components, members of globular clusters, are discussed in Section 6. Finally, Section 7 summarizes our results.

2. Observations and Data Reduction

The OGLE photometric observations used in this work were carried out with the 1.3-m Warsaw telescope at Las Campanas Observatory, Chile, between 2013 and 2020. The field of view of an OGLE CCD mosaic camera is 1.4 square degrees and the pixel scale is $0\farcs26$. The telescope is equipped with two filters, *I*- and *V*-bands, closely resembling Cousins-Johnson standard photometric systems.

Details of the OGLE instrumentation and data reduction procedures can be found in Udalski *et al.* (2015a, 2018).

The OGLE GVS project covers approximately 3000 square degrees along the Galactic plane, from Galactic longitudes of about -170° to $+60^\circ$ and latitudes from -7° to $+7^\circ$ in the disk and from -15° to $+15^\circ$ in the bulge region. This is a shallower survey than the regular OGLE project, with 25 s and 30 s integration times for *I*-band and *V*-band, respectively (compared to 100–150 s for the regular OGLE observations).

Until March 2020, when the Warsaw telescope was temporarily closed due to the COVID-19 pandemic, between 100 and 200 *I*-band epochs per star have been acquired for the majority of the GVS fields. Time span of individual light curves range from 2 yr to 7 yr. The *V*-band observations (usually several epochs) are currently available for approximately half of the stars.

3. Selection and Classification of δ Sct Stars

Our search for Galactic δ Sct stars was very similar to the search for RR Lyr stars and Cepheids in the same fields (Udalski *et al.* 2018, Soszyński *et al.* 2019, 2020). In the first step, over 1 billion point sources in the outer bulge and Galactic disk photometrically monitored by the OGLE GVS were subjected to a Fourier-based frequency analysis with the FNPEAKS code [‡]. The probed frequency space ranged from 0 to 30 cycles per day, with a step of $5 \cdot 10^{-5}$ cycles per day. For each analyzed time series, the FNPEAKS code returned 10 most significant periodicities with their signal-to-noise ratios. Then, each light curve was prewhitened with the primary frequency and its harmonics and the period search was repeated on the residuals.

In the second step, we performed a visual inspection of *I*-band light curves with the primary periods below 0.3 d and the highest signal-to-noise ratios. In this way, we divided our targets into three groups: candidates for pulsating stars, eclipsing and ellipsoidal binaries, and other (usually unknown) types of variable stars. Our classification criteria were mainly based on the morphology of the light curves, in particular we required an asymmetry seen in the phased light curve to consider a star as a pulsator. However, the above condition was not applied to multiperiodic pulsating variables – in these cases we primarily relied on their characteristic period ratios (see Section 6.2) and their position in the Petersen diagram (where the shorter-to-longer period ratio is plotted against the logarithm of the longer period).

In the last step of our procedure, we isolated probable δ Sct variables from the list of candidate pulsating stars. Since there is a continuity between δ Sct stars and classical Cepheids, we adopted a period of 0.23 d of the first-overtone mode (corresponding to about 0.3 d for the fundamental mode) to separate both classes of pulsators. The distinction between long-period ($P > 0.2$ d) δ Sct stars and short-

[‡] *http://helas.astro.uni.wroc.pl/deliverables.php?lang=en&active=fnpeaks*

period ($P < 0.3$ d) overtone RR Lyr stars is not obvious. Most of the single-mode pulsating stars with periods in this range were recognized as RRc variables and published in the OGLE collection of RR Lyr stars (Soszyński *et al.* 2019). On the other hand, multimode variables with these periods were mostly classified as δ Sct stars, because double-mode RR Lyr (RRd) stars generally have longer periods and different period-ratios. Finally, we carefully checked and rejected most of the stars with $(V-I)$ color index below 0.2 mag, since such blue objects probably belong to the β Cephei class of pulsating variables. However, it cannot be ruled out that a number of β Cep stars with the colors reddened by a strong interstellar extinction remained in our list. Spectroscopic observations are required to ultimately distinguish β Cep from δ Sct pulsators.

Similarly, the division of δ Sct variables into Population I and Population II (SX Phe) stars requires complex studies of their evolutionary status and is beyond the scope of this paper. The distinction between δ Sct and SX Phe stars is not possible on the basis of their amplitudes or number of frequencies (Balona and Nemec 2012), also there is no boundary period that can be used to separate both populations, although SX Phe stars have on average shorter periods than their younger counterparts (Jayasinghe *et al.* 2020). There are also difficulties in unambiguously identifying the pulsation modes in some individual δ Sct stars, so we decided not to provide mode classification in our collection. Instead, we split our sample into singlemode and multimode variables. The latter group contains objects with well-defined secondary periods that can be associated with additional radial or nonradial pulsation modes.

In total, we distinguished 14 328 likely Galactic δ Sct stars that were not included in the previously published parts of the OCVS (Pietrukowicz *et al.* 2013, 2020). This sample has enlarged our collection of δ Sct variables in the Milky Way by 140%, and currently this is the largest catalog of such stars.

4. The OGLE Collection of Galactic δ Sct Stars

The newly detected δ Sct stars in the Galactic bulge and disk have been added to the already published parts of the OCVS (Pietrukowicz *et al.* 2013, 2015, 2020). Currently, the full collection contains 24 488 δ Sct stars divided into 18 638 single-mode and 5850 multimode pulsators. 16 812 of these stars have been found in the bulge region, while 7676 objects are located in the Galactic disk[§]. All sources are available online at the OGLE Internet Archive:

http://ogle.astrouw.edu.pl > OGLE Collection of Variable Stars
http://www.astrouw.edu.pl/ogle/ogle4/OCVS/blg/dsct/
http://www.astrouw.edu.pl/ogle/ogle4/OCVS/gd/dsct/

[§]The bulge and disk OGLE fields are shown in the maps on the OGLE website.

The identifiers of our δ Sct stars follow the scheme introduced by Pietrukowicz *et al.* (2013, 2020): OGLE-BLG-DSCT-XXXXX and OGLE-GD-DSCT-YYYY for bulge and disk populations, respectively, where XXXXX and YYYY are consecutive numbers. The new samples are arranged according to their equinox equatorial coordinates ordered by increasing right ascension. For each star, we provide its equatorial coordinates (J2000.0), intensity-averaged mean magnitudes in the *I*- and *V*-bands (if available), and up to three dominant periods with the corresponding amplitudes, epochs of the maximum light, and Fourier coefficients. The pulsation periods have been refined with the TATRY code (Schwarzenberg-Czerny 1996). For the previously known variables, we give their designations from the International Variable Star Index (VSX, Watson *et al.* 2006).

The OGLE *I*- and *V*-band time-series photometry collected during the OGLE-II, OGLE-III, and OGLE-IV projects (if available) have been provided for the entire sample, so the time span of the light curves may reach 23 yr (1997–2020) for some δ Sct stars. The photometric data from each phase of the OGLE project have been independently calibrated to the standard Johnson-Cousins photometric system. However, note that small offsets between the photometric zero points may occur for individual objects, which can be a result of crowding and blending by unresolved stars or different instrumental configurations during the three phases of the OGLE survey. These zero-point shifts should be compensated before merging the light curves from different stages of the project.

Fig. 1 shows on-sky maps of our collection of δ Sct stars. The upper panel presents a surface density map in a square root scaling. The best-populated fields in the Galactic bulge contain over 200 δ Sct variables per square degree, while around the Galactic anticenter we found on average only 2.7 δ Sct stars per square degree. Additionally, there is a deficit of variables close to the Galactic plane in the bulge region, which is due to the enormous interstellar extinction in these directions.

The middle and lower panels of Fig. 1 show positions of individual δ Sct stars plotted over the OGLE-IV footprint. Different colors of the points refer to different mean *I*-band magnitudes and different dominant pulsation periods for middle and lower panels, respectively. Both distributions are not homogeneous. The distribution of magnitudes (middle panel of Fig. 1) primarily shows the map of interstellar matter close to the Galactic plane, while the period distribution (lower panel of Fig. 1) primarily reflects the metallicity gradient in the Milky Way.

As can be seen by inspection of the lower panel of Fig. 1, stars located farther from the Galactic equator have generally shorter periods, which is especially noticeable in the bulge region. Jayasinghe *et al.* (2020) noticed that metal-poor δ Sct stars have on average shorter pulsation periods than metal-rich variables, so the visible period gradient can be useful for distinguishing between Population II SX Phe stars (members of the spheroidal component of the Milky Way) and Population I δ Sct variables (disk members).

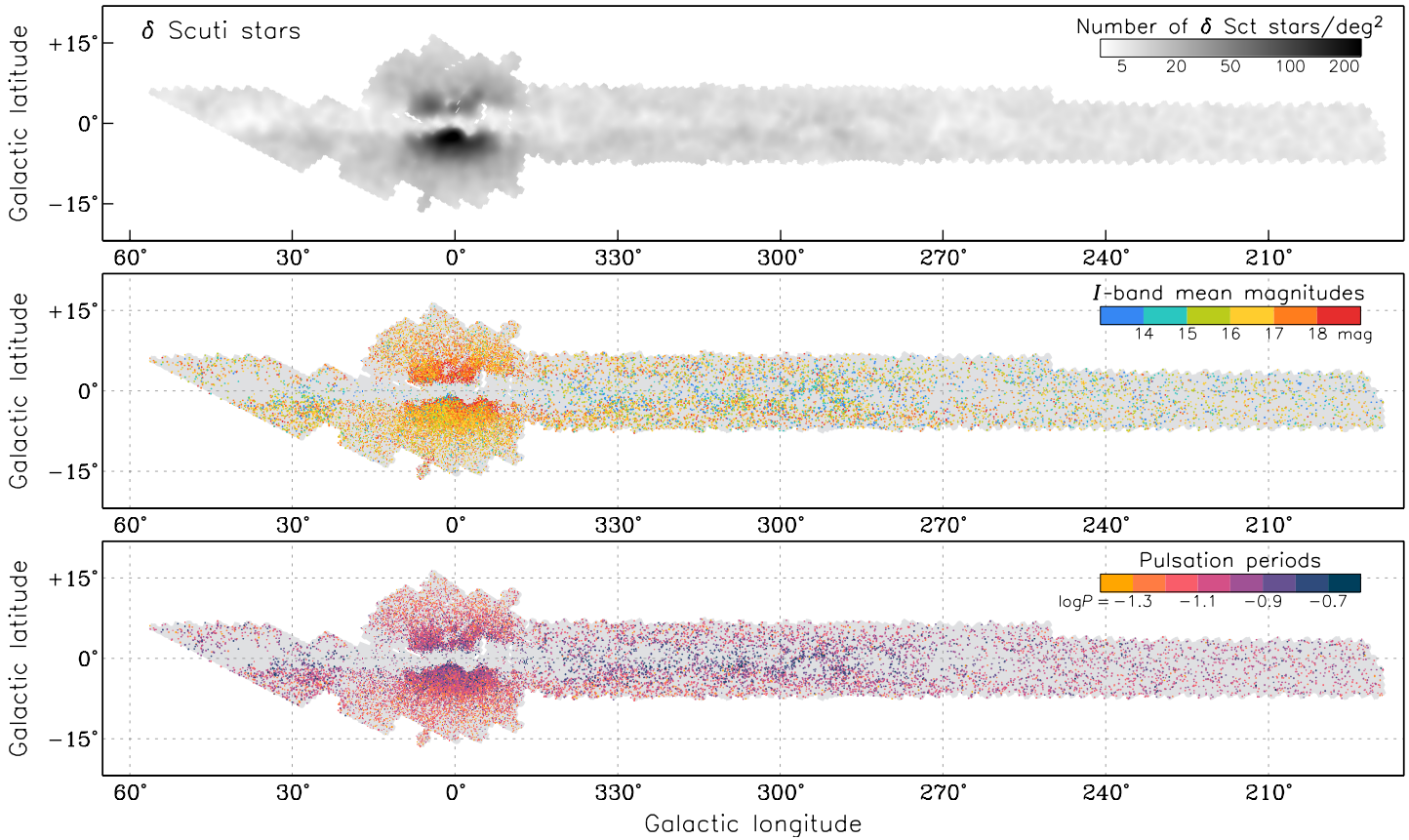

Fig. 1. On-sky distributions of δ Sct stars in the Galactic coordinates. *Upper panel* displays a surface density map in a square root scaling. *Middle* and *lower panels* show positions of individual objects with colors of the points coding *I*-band mean magnitudes and dominant pulsation periods, respectively. The gray area shows the OGLE footprint in the Galactic bulge and disk.

5. Completeness and Cross-Check with Other Catalogs

We cross-matched our collection of Galactic δ Sct stars with several catalogs of variable stars to check the accuracy of our classification and the completeness of our sample. In the VSX, ASAS-SN and ZTF catalogs of variable stars (Watson *et al.* 2006, Jayasinghe *et al.* 2020, Chen *et al.* 2020) we found a total of 1757 out of 14 328 newly selected δ Sct stars. The great majority of these previously known stars have been classified as δ Sct variables (DSCT, HADS, or SXPHE) in the external catalogs. However, several dozen objects were assigned to other categories, usually contact binary systems or RR Lyr stars. We verified these stars by re-inspecting their OGLE light curves and in some cases we changed our classification removing these objects from our sample.

On the other hand, the VSX, ASAS-SN, and ZTF catalogs contain over 1500 objects classified as δ Sct stars that were not included in the preliminary version of our collection, despite the fact that their time-series photometry was available in the OGLE database. We carefully examined these light curves and completed our collection with 159 additional δ Sct variables that were overlooked in our selection procedure. The rest of the candidates for δ Sct stars from other surveys turned out to be eclipsing or ellipsoidal binaries, low-amplitude variables of vague type, or just constant stars. Some of the low-amplitude variables with sinusoidal light curves may actually be δ Sct pulsators, however we decided not to add these stars to our collection, because their classification was very uncertain.

The completeness of our collection of δ Sct stars was assessed based on the objects with two entries in the OGLE database due to their position in the overlapping parts of adjacent OGLE fields. We had the potential to double-detect these objects during our selection procedure, although the final version of the collection contains only one entry per star – usually the one with a larger number of data points. Considering only light curves with 30 or more data points, we *a posteriori* detected 712 stars with double detections in the OGLE database, so we had a chance to find 1424 counterparts. We independently identified 1163 of them, which corresponds to the completeness of about 78%.

This moderate completeness reflects the difficulties of identifying δ Sct stars with small amplitudes and symmetric light curves. In contrast to Cepheids or RR Lyr stars, the number of δ Sct variables increases with decreasing amplitudes. Indeed, most of the missed objects belong to the lowest-amplitude ($A(I) <$ 0.1 mag) pulsators in our collection. We also checked the completeness of the sample of high-amplitude δ Sct stars (HADS) with the *I*-band amplitudes larger than 0.3 mag. As expected, the completeness of the HADS collection was much higher, reaching 90%. In this case, the overlooked objects were almost exclusively the weakest ones, with *I*-band mean magnitudes greater than 18 mag.

6. Discussion

6.1. Period, Magnitude, and Amplitude Distributions

Fig. 2 displays the distributions of dominant pulsation periods (upper panel), apparent *I*-band mean magnitudes (middle panel), and *I*-band peak-to-peak amplitudes (lower panel) of 24 488 δ Sct stars from our collection. In addition to the total sample (green histograms), we present the distributions separately for δ Sct variables found toward the Galactic bulge (red histograms) and toward the Galactic disk (blue histograms).

The distribution of pulsation periods of the total sample has a double maximum: for periods of about 0.063 d ($\log P = -1.20$) and 0.085 d ($\log P = -1.07$). The former value corresponds to the peak in the period distribution for the bulge δ Sct population, while the latter period coincides with the maximum of the distribution for the disk variables. These evidently different period distributions of δ Sct stars in the bulge and disk must be related to their different evolutionary history. The shorter-period metal-poor SX Phe stars seem to be much more common in the central parts of the Milky Way, while Population I δ Sct stars dominate in the Galactic disk.

The bulge and disk members also have different luminosity distributions (middle panel of Fig. 2). In this case, it can be explained by the different depths of the regular and GVS OGLE surveys. The bulge sample is largely composed of the δ Sct stars detected by Pietrukowicz *et al.* (2020) in the regular OGLE fields, where the faintest objects reach luminosities of $I > 20$ mag. The disk variables were mostly identified in the shallower GVS dataset, so the faintest stars in this sample barely exceed $I = 19$ mag. On the other hand, the saturation limit is respectively brighter in the GVS photometry, up to $I = 11$ mag.

The amplitude distribution (lower panel of Fig. 2) peaks at $A(I) \approx 0.12$ mag. It can be assumed that the completeness of our collection decreases toward smaller amplitudes and completely collapses for amplitudes below 0.04 mag. It is interesting that the amplitude distribution for the disk sample of δ Sct stars has a maximum at $A(I) \approx 0.05$ mag, which probably indicates that there is potential to increase the completeness of our bulge sample.

6.2. Multimode Variables

Multiperiodic δ Sct stars are useful in asteroseismological studies, because two or more accurately measured pulsation modes yield strong constraints on the stellar mass, luminosity, and chemical composition. Recently, Netzel *et al.* (2021) studied the OGLE collection of 10 092 δ Sct stars in the Galactic bulge (Pietrukowicz *et al.* 2020) and identified 3083 objects pulsating in two, three or even four radial modes simultaneously. The characteristic period ratios of the radial modes were used for their identification. Additionally, a large fraction of δ Sct variables exhibit nonradial pulsation modes (*e.g.*, Pietrukowicz *et al.* 2015), which, however, are far

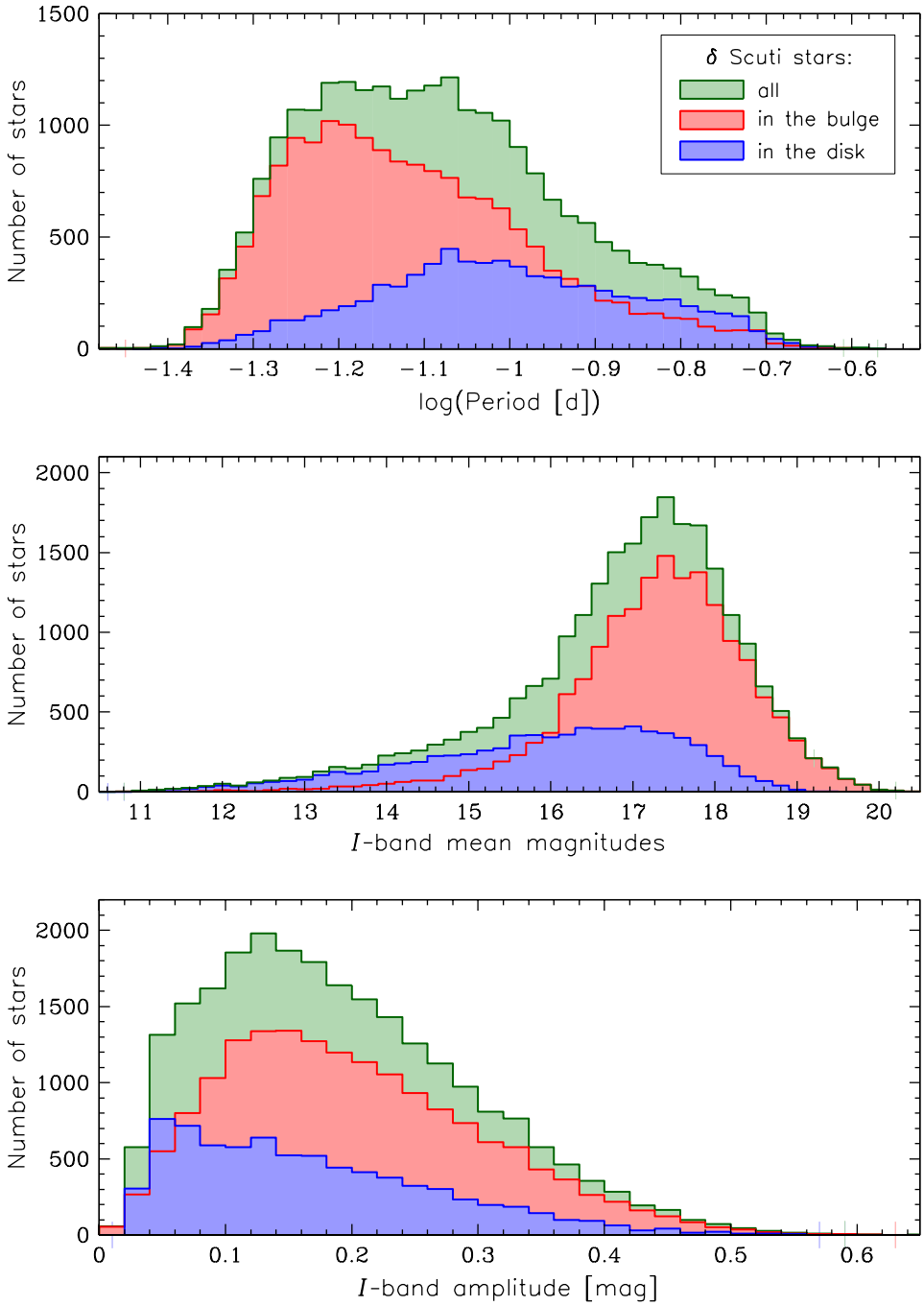

Fig. 2. Distributions of dominant pulsation periods (*upper panel*), *I*-band mean magnitudes (*middle panel*), and *I*-band peak-to-peak amplitudes (*lower panel*) of δ Sct stars in the Milky Way. Red histograms show 16 812 variables identified in the fields toward the Galactic bulge, blue histograms show distributions of 7676 objects detected in the Galactic disk, green histograms are the sum of the previous two.

more difficult to identify, because they may form a variety of period ratios with other modes.

We performed a search for multiperiodic δ Sct stars using the standard method. From each *I*-band light curve, the dominant frequency and its harmonics were subtracted by fitting a truncated Fourier series. Then, the period search was conducted on the residual data and the process of the light curve prewhitening and frequency analysis was repeated. Finally, we visually inspected the light curves with the largest signal-to-noise ratios of the secondary and tertiary periods. In this way, we selected only the stars with the most distinct additional periodicities. Thus, the completeness of our sample of multimode δ Sct pulsators can be improved by including periodicity associated with smaller amplitudes, but at the cost of lower purity of the sample.

Fig. 3 shows the Petersen diagram for the detected multimode δ Sct stars. Red and blue points indicate objects found in the Galactic bulge and disk regions, re-

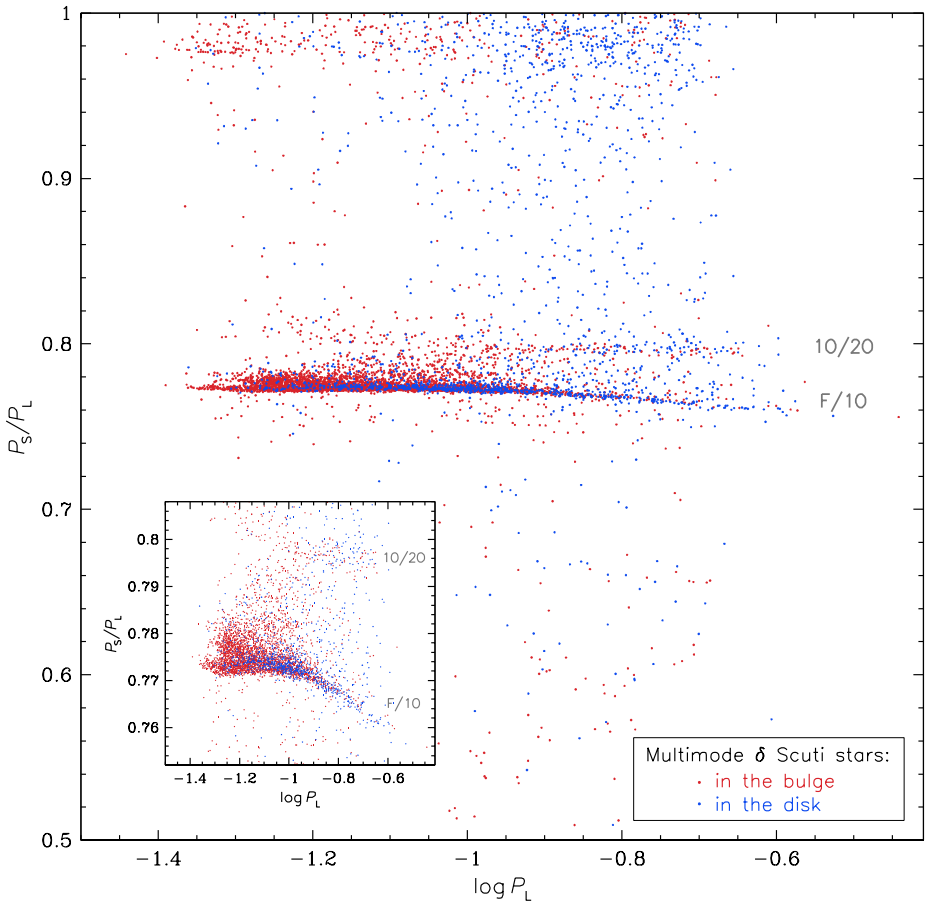

Fig. 3. Petersen diagram for multimode δ Sct stars in the Galactic bulge (red points) and disk (blue points). The inset shows a zoom-in to the sequences formed by F/1O and 1O/2O variables.

spectively. The bulge variables have on average shorter periods, but generally both populations follow the same sequences in the Petersen diagram. The most conspicuous structure in this diagram is the sequence for period ratios ranging from ≈ 0.76 to ≈ 0.78 formed by the fundamental (F) and first-overtone (1O) pulsation modes. The second sequence at ≈ 0.80 period ratios corresponds to the first and second (2O) overtones. Both sequences are zoomed in the inset in Fig. 3 to reveal details of these structures. Note, for example, that the F/1O sequence splits into two branches in the short-period end: for periods ratios of about 0.773 and 0.778.

Approximately a third of the selected multiperiodic δ Sct stars are located outside the F/1O and 1O/2O sequences in the Petersen diagram. This group includes nonradial pulsators as well as double-, triple-, or even quadruple-mode pulsators (Netzel *et al.* 2021) with various combinations of the radial modes excited. The former category includes stars with a close pair of frequencies, which are visible as a surplus of points at the top of the Petersen diagram ($P_S/P_L \gtrsim 0.95$). The most plausible explanation for these close doublets of frequencies is the excitation of nonradial modes by resonance with the main period of oscillation.

The identification of the pulsation modes is not a simple task for many δ Sct variables, therefore we do not include this information in our collection. We just divide our sample into singlemode and multimode pulsators and provide up to three dominant periods for each star.

6.3. δ Sct Stars in Binary Systems

Binary systems with oscillating components are powerful tools for probing the absolute stellar parameters of the pulsating stars: masses, radii, and luminosities. Known binaries containing δ Sct stars are much more common than systems containing classical Cepheids (*e.g.*, Udalski *et al.* 2015b, Pilecki *et al.* 2021) or RR Lyr stars (*e.g.*, Hajdu *et al.* 2021). Kahraman Aliçavuş *et al.* (2017) published a list of 92 eclipsing binary systems with a δ Sct component, while Liakos and Niarchos (2017) cataloged as many as 199 eclipsing, ellipsoidal, visual, and spectroscopic binaries containing δ Sct stars.

Binary systems with δ Sct components are also present in our collection. Pietrukowicz *et al.* (2020) listed 14 δ Sct variables with additional eclipsing or ellipsoidal modulation. In this paper, we expand this list with additional 20 systems. We divided this sample into detached systems, semidetached systems and ellipsoidal variables. Table 1 provides the most important parameters of these objects, while Fig. 4 shows light curves of six objects from this sample.

In addition, we found five δ Sct stars with well pronounced secondary periods in the range 2–4 d, for which we did not detect alternating shallower and deeper minima characteristic for ellipsoidal variables (Fig. 5, Table 2). We do not rule out that these long-period modulations are caused by binarity (in such case the orbital periods would be twice as long as the measured ones), but it might be also changes

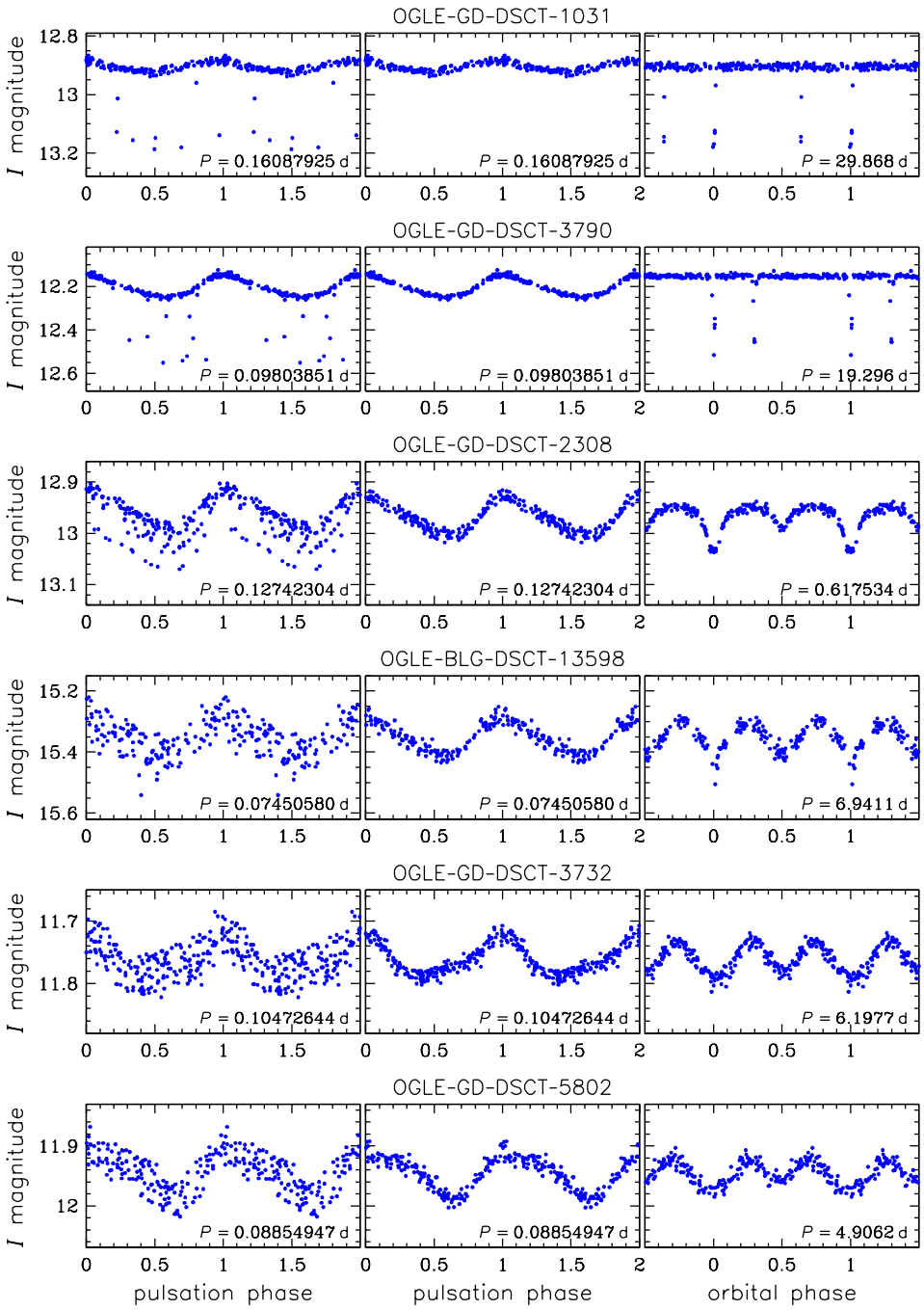

Fig. 4. Example *I*-band light curves of δ Sct stars with additional eclipsing (four *upper panels*) or ellipsoidal (two *lower panels*) modulation. *Left panels* show original light curves folded with the pulsation periods. *Middle* and *right panels* present pulsation and eclipsing/ellipsoidal light curves, respectively, after subtracting the other component.

T a b l e 1

New δ Sct stars with additional eclipsing or ellipsoidal modulation

Identifier	R.A. [J2000.0]	Dec. [J2000.0]	$\langle I \rangle$ [mag]	$P_{\rm puls}$ [d]	$P_{\rm orb}$ [d]	Binarity type
OGLE-GD-DSCT-0393	$06^{\rm h}34^{\rm m}28\overset{\rm s}{.}31$	$+09°23'38\overset{''}{.}2$	13.755	0.06005839	4.9618	EA
OGLE-GD-DSCT-1031	$07^{\rm h}31^{\rm m}39\overset{\rm s}{.}71$	$-28°45'05\overset{''}{.}9$	12.919	0.16087925	29.868	EA
OGLE-GD-DSCT-1398	$08^{\rm h}00^{\rm m}23\overset{\rm s}{.}53$	$-23°35'35\overset{''}{.}5$	14.081	0.14320227	5.0375	EA
OGLE-GD-DSCT-1423	$08^{\rm h}03^{\rm m}11\overset{\rm s}{.}27$	$-36°47'52\overset{''}{.}9$	14.560	0.11235700	18.567	EA
OGLE-GD-DSCT-2308	$09^{\rm h}45^{\rm m}56\overset{\rm s}{.}82$	$-59°50'41\overset{''}{.}9$	12.968	0.12742304	0.617534	EB
OGLE-GD-DSCT-3010	$11^{\rm h}04^{\rm m}00\overset{\rm s}{.}73$	$-56°39'04\overset{''}{.}6$	13.050	0.08425622	7.4180	Ell
OGLE-GD-DSCT-3494	$12^{\rm h}05^{\rm m}49\overset{\rm s}{.}30$	$-58°32'49\overset{''}{.}4$	15.390	0.08109499	6.2934	Ell
OGLE-GD-DSCT-3732	$12^{\rm h}36^{\rm m}23\overset{\rm s}{.}93$	$-58°58'20\overset{''}{.}2$	11.760	0.10472644	6.1977	Ell
OGLE-GD-DSCT-3790	$12^{\rm h}44^{\rm m}18\overset{\rm s}{.}26$	$-66°40'29\overset{''}{.}0$	12.224	0.09803851	19.296	EA
OGLE-GD-DSCT-5612	$16^{\rm h}08^{\rm m}36\overset{\rm s}{.}57$	$-55°51'11\overset{''}{.}2$	14.310	0.07350542	3.1868	EB
OGLE-GD-DSCT-5802	$16^{\rm h}20^{\rm m}54\overset{\rm s}{.}45$	$-54°55'19\overset{''}{.}4$	11.946	0.08854947	4.9062	Ell
OGLE-GD-DSCT-5901	$16^{\rm h}27^{\rm m}08\overset{\rm s}{.}32$	$-40°46'36\overset{''}{.}6$	16.681	0.08709063	3.4373	EB
OGLE-GD-DSCT-5979	$16^{\rm h}32^{\rm m}26\overset{\rm s}{.}61$	$-53°11'11\overset{''}{.}2$	15.758	0.07376154	6.6009	Ell
OGLE-GD-DSCT-6092	$16^{\rm h}39^{\rm m}21\overset{\rm s}{.}85$	$-45°46'26\overset{''}{.}7$	14.530	0.11055747	8.8291	Ell
OGLE-GD-DSCT-6454	$17^{\rm h}12^{\rm m}13\overset{\rm s}{.}12$	$-50°29'24\overset{''}{.}5$	14.299	0.08480399	5.5759	Ell
OGLE-GD-DSCT-6772	$18^{\rm h}43^{\rm m}11\overset{\rm s}{.}85$	$-08°45'22\overset{''}{.}6$	15.734	0.07839580	3.6596	Ell
OGLE-BLG-DSCT-11682	$17^{\rm h}15^{\rm m}33\overset{\rm s}{.}49$	$-17°06'37\overset{''}{.}3$	16.344	0.05725150	2.8922	Ell
OGLE-BLG-DSCT-13598	$17^{\rm h}55^{\rm m}27\overset{\rm s}{.}56$	$-37°54'38\overset{''}{.}6$	15.352	0.07450581	6.9411	EB
OGLE-BLG-DSCT-14775	$18^{\rm h}23^{\rm m}04\overset{\rm s}{.}05$	$-29°21'24\overset{''}{.}0$	15.967	0.05889860	3.7133	Ell
OGLE-BLG-DSCT-16533	$18^{\rm h}49^{\rm m}50\overset{\rm s}{.}75$	$-16°46'06\overset{''}{.}7$	13.889	0.08021462	5.1894	Ell

T a b l e 2

δ Sct stars with additional long-term modulation

Identifier	R.A. [J2000.0]	Dec. [J2000.0]	$\langle I \rangle$ [mag]	$P_{\rm puls}$ [d]	$P_{\rm long}$ [d]
OGLE-GD-DSCT-4292	$13^{\rm h}47^{\rm m}34\overset{\rm s}{.}65$	$-64°09'00\overset{''}{.}7$	16.111	0.08243829	3.6354
OGLE-GD-DSCT-6291	$16^{\rm h}52^{\rm m}20\overset{\rm s}{.}90$	$-50°01'54\overset{''}{.}3$	15.619	0.07778187	2.6947
OGLE-GD-DSCT-7030	$18^{\rm h}52^{\rm m}58\overset{\rm s}{.}95$	$-07°34'13\overset{''}{.}9$	15.363	0.08036922	2.9303
OGLE-GD-DSCT-7462	$19^{\rm h}07^{\rm m}01\overset{\rm s}{.}75$	$+14°02'37\overset{''}{.}6$	14.549	0.08858910	3.5932
OGLE-BLG-DSCT-16754	$19^{\rm h}00^{\rm m}30\overset{\rm s}{.}22$	$-15°08'30\overset{''}{.}0$	15.266	0.08736216	2.2873

caused by the rotation of spotted stars or by nonradial oscillations as γ Doradus stars. Such hybrid δ Sct/γ Dor variables are well known (*e.g.*, Henry and Fekel 2005) and it is no wonder that they could also appear in our collection.

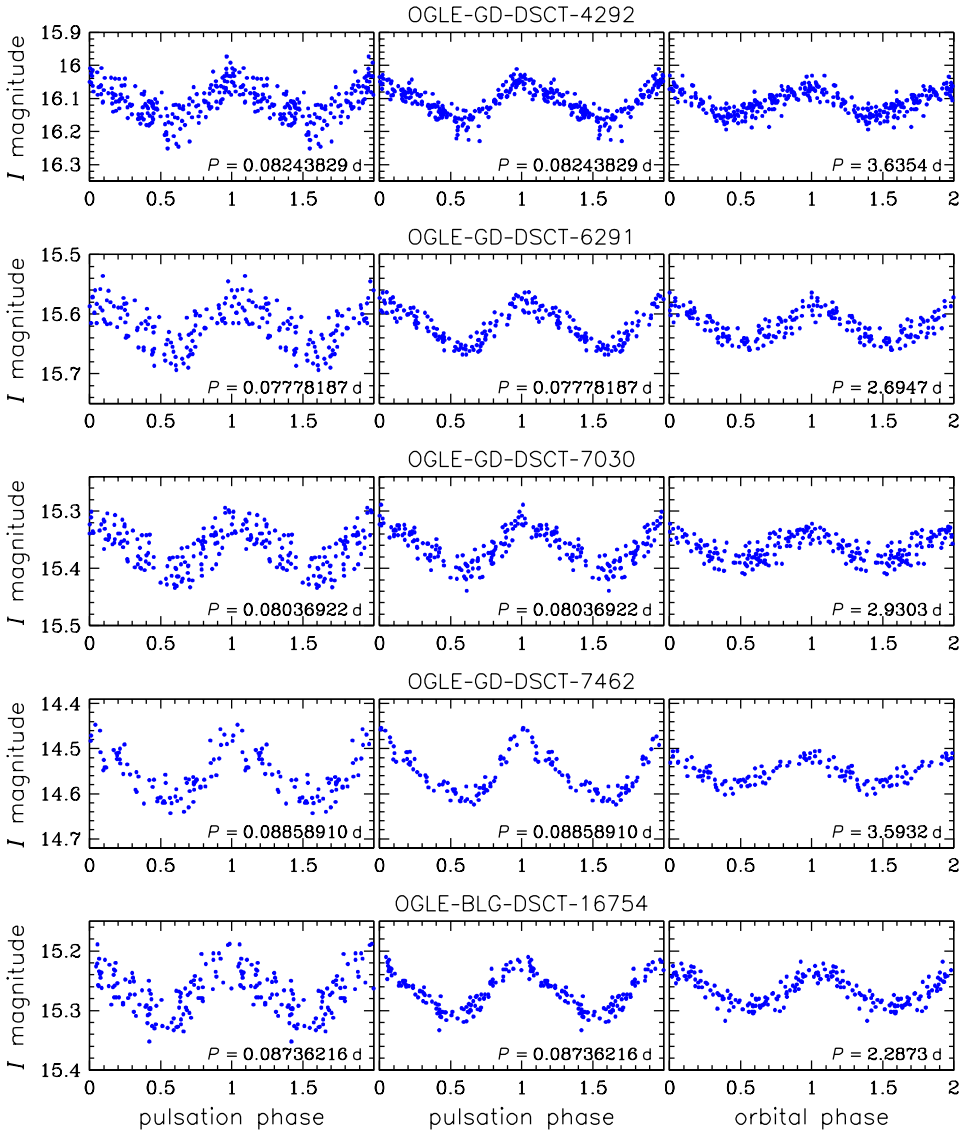

Fig. 5. *I*-band light curves of δ Sct stars with additional long-period modulation. *Left panels* show original light curves folded with the pulsation periods. *Middle* and *right panels* show disentangled light curves folded with the pulsation and long period, respectively.

6.4. Globular Clusters Members

Among over 10 000 δ Sct variables detected toward the Galactic bulge, Pietrukowicz *et al.* (2020) distinguished 22 objects that are located in the sky not farther than three half-light radii ($3r_h$) from the centers of nine globular clusters. Most of these stars are probably SX Phe variables that are cluster members, but some of them may be field objects accidentally located along the same line-of-sight as the cluster.

T a b l e 3

δ Sct stars located within the radius of $3r_h$ from centers of globular clusters

Cluster	Identifier	$\langle I \rangle$	$P_{\rm puls}$	r/r_h	Other name
M62	OGLE-BLG-DSCT-10730	16.357	0.09267790	0.4	
M19	OGLE-BLG-DSCT-10810	17.536	0.06571908	1.1	
NGC 6287	OGLE-BLG-DSCT-10961	17.835	0.06571120	0.5	
Ton 2	OGLE-BLG-DSCT-12743	17.767	0.14461103	2.6	
	OGLE-BLG-DSCT-12754	18.368	0.11930232	1.8	
NGC 6441	OGLE-BLG-DSCT-13369	16.702	0.08992963	2.6	V1517 Sco
NGC 6541	OGLE-BLG-DSCT-14113	16.547	0.05746375	1.5	
	OGLE-BLG-DSCT-14119	16.149	0.06466907	0.1	V0825 CrA
	OGLE-BLG-DSCT-14120	16.180	0.06571376	0.3	V0826 CrA
NGC 6558	OGLE-BLG-DSCT-14210	16.777	0.06851215	1.4	
M28	OGLE-BLG-DSCT-14983	17.234	0.06551779	2.8	
NGC 6638	OGLE-BLG-DSCT-15476	16.825	0.05766997	2.2	

In this work, we extend this list by additional 12 δ Sct (SX Phe) stars positionally coincident with nine globular clusters. In Table 3, we present these variables found in the regions outlined by three half-light radii of the clusters. We used this condition to comply with the work by Pietrukowicz *et al.* (2020), however different criteria would result in significantly different numbers of candidate cluster members. For example, as many as 71 δ Sct variables are located within one tidal radius from the center of a globular cluster. Future investigations, in particular analysis of their proper motions, should answer the question of how many of these stars are physically associated with the clusters.

7. Conclusions

We release the largest sample of δ Sct stars in the Milky Way. Our collection includes about 10 000 variables identified by Pietrukowicz *et al.* (2020) in the OGLE Galactic bulge fields and over 14 000 new objects detected in the GVS fields in the Galactic disk and outer bulge. The vast majority ($\sim$88%) of these new δ Sct stars have not been reported by other sky surveys so far. For each object, we provide its long-term OGLE light curves spanning over 20 years (OGLE-II + OGLE-III + OGLE-IV) in some cases. These data are available through a user-friendly WWW interface. Our collection provides a framework for better understanding of pulsations and evolution of intermediate-mass stars.

Acknowledgements. This work has been supported by the National Science Centre, Poland, grant MAESTRO no. 2016/22/A/ST9/00009. MG is supported by

the EU Horizon 2020 research and innovation programme under grant agreement No 101004719. This research has made use of the International Variable Star Index (VSX) database, operated at AAVSO, Cambridge, Massachusetts, USA.

REFERENCES

Balona, L.A. and Nemec, J.M. 2012, *MNRAS*, **426**, 2413.
Chen, X., Wang, S., Deng, L., *et al.* 2020, *ApJS*, **249**, 18.
Hajdu, G., Pietrzyński, G., Jurcsik, J., *et al.* 2021, *ApJ*, **915**, 50.
Henry, G.W., and Fekel, F.C. 2005, *AJ*, **129**, 2026.
Jayasinghe, T., Stanek, K.Z., Kochanek, C.S., *et al.* 2020, *MNRAS*, **493**, 4186.
Kahraman Aliçavuş, F., Soydugan, E., Smalley, B., and Kubát, J. 2017, *MNRAS*, **470**, 915.
Liakos, A., and Niarchos, P. 2017, *MNRAS*, **465**, 1181.
Netzel, H., Pietrukowicz, P., Soszyński, I., and Wrona, M. 2021, arXiv:2107.08064.
Pietrukowicz, P., Dziembowski, W.A., Mróz, P. *et al.* 2013, *Acta Astron.*, **63**, 379.
Pietrukowicz, P., Latour, M., Angeloni, R., *et al.* 2015, *Acta Astron.*, **65**, 63.
Pietrukowicz, P., Soszyński, I., Netzel, H., *et al.* 2020, *Acta Astron.*, **70**, 241.
Pilecki, B., Pietrzyński, G., Anderson, R.I., *et al.* 2021, *ApJ*, **910**, 118.
Rodríguez, E., López-González, M.J., and López de Coca, P. 2000, *A&AS*, **144**, 469.
Schwarzenberg-Czerny, A. 1996, *ApJ*, **460**, L107.
Soszyński, I., Udalski, A., Wrona, M., *et al.* 2019, *Acta Astron.*, **69**, 321.
Soszyński, I., Udalski, A., Szymański, M.K., *et al.* 2020, *Acta Astron.*, **70**, 101.
Udalski, A., Szymański, M.K., and Szymański, G. 2015a, *Acta Astron.*, **65**, 1.
Udalski, A., Soszyński, I., Szymański, M.K., *et al.* 2015b, *Acta Astron.*, **65**, 341.
Udalski, A., Soszyński, I., Pietrukowicz, P., *et al.* 2018, *Acta Astron.*, **68**, 315.
Watson, C.L., Henden, A.A., and Price, A. 2006, The Society for Astronomical Sciences 25th Annual Symposium on Telescope Science, p. 47.